PHYSICS BASED TARGET DETECTION USING A HYBRID ALGORITHM WITH AN INFEASIBILITY METRIC

Emmett J. Ientilucci and John R. Schott

Digital Imaging and Remote Sensing Laboratory, Rochester Institute of Technology
54 Lomb Memorial Drive, Rochester, NY 14623-5604
emmett@cis.rit.edu, schott@cis.rit.edu

ABSTRACT

This paper develops (and applies) a hybrid target detector that incorporates structured backgrounds and physics based modeling together with a geometric infeasibility metric. More often than not, detection algorithms are usually applied to atmospherically compensated hyperspectral imagery. Rather than compensate the imagery, we take the opposite approach by using a physics based model to generate permutations of what the target might look like as seen by the sensor in radiance space. The development and status of such a method is presented and applied to the generation of target spaces. The generated target spaces are designed to fully encompass image target pixels while using a limited number of input model parameters. Additionally, a Structured Infeasibility Projector (SIP) is developed which enables one to be more selective in rejecting false alarms. Results on HYDICE data show that the SIP algorithm, in conjunction with a physics based detector, outperforms results from the SAM and SMF algorithms for a target that is both fully sunlit and obscured by a tree canopy.

1. INTRODUCTION

This paper investigates a geometric hybrid technique for the detection of subpixel targets in uncompensated image spectrometer data. Physical models are used to predict what the sensor-reaching radiance looks like based on direct solar illumination, upwelled and downwelled radiances as well as reflectivity of the target. This approach uses an atmospheric propagation model to produce an illumination invariant (radiance) target space that can be used in the detection scheme outlined in this paper.

The approach we take throughout this research is geometric or structured in nature. Therefore, in developing our hybrid algorithm, we describe the background data using a linear subspace approach characterized by endmembers. We then present a detector that tells us how much influence the background space has on an image pixel. The output of such a detector is an abundance-like term where large values are synonymous with targets. In general, however, the output of the detector may produce large values, not only for actual targets, but for any other spectral anomaly that has a significant projection (*e.g.,* a bright or saturated pixel) thus producing false alarms. Geometrically, we recognize where these cases can occur. We note that there exists many different image pixels that can have the same background influence or abundance. These pixels may manifest themselves as false positives. We separate such pixels through incorporation of an operator called the Structured Infeasibility Projector (SIP) which is applied to a physically derived target space. Together, the detector and SIP form a hybrid algorithm called the Physics Based-Structured InFeasibility Target-detector (PB-SIFT). The detector's performance is demonstrated by comparing the hybrid algorithm to the spectral angle mapper (SAM) and spectral matched filter (SMF) detectors. These algorithms are applied to HYDICE imagery. Analysis is made through use of Receiver Operating Characteristic (ROC) curves.

This work was funded under the Office of Naval Research Multidisciplinary University Research Initiative "Model-based Hyperspectral Exploitation Algorithm Development" #N00014-01-1-0867

2. BACKGROUND AND THEORY

2.1. Physics Based Modeling(PBM) and Target Spaces

In target detection, we often seek to atmospherically compensate hyperspectral imagery so as to convert sensor reaching radiance to ground leaving spectral reflectance. Once the imagery has been compensated, detection algorithms are used to compare image reflectances to library or measured reflectances in search of a desired target. Rather than compensate the imagery, an alternative is to estimate what the ground leaving spectral reflectance would look like as seen by the sensor in radiance space [1]. This approach entails modeling the propagation of a target reflectance spectrum through the atmosphere up to the sensor. The advantage this technique has over that of compensated imagery is that target illumination variations can be integrated into the process through use of a physical model thus making the approach *invariant* to illumination effects. Schott [2] derives such a physical model for the spectral radiance reaching an airborne or satellite sensor which incorporates direct illumination variation as well as downwelling and upwelling (or path) radiance. This can be expressed in simplified form as

$$L_p(\lambda) = \int_\lambda \beta_p(\lambda)\Bigg[\Big(E_s'(\lambda)\tau_1(\lambda)\cos\theta + FE_d(\lambda)\Big)\tau_2(\lambda)\frac{r(\lambda)}{\pi} + L_u(\lambda)\Bigg]d\lambda \qquad (1)$$

where $L_p(\lambda)$ is the effective spectral radiance in the p^{th} band in units of $[Wcm^{-2}sr^{-1}\mu m^{-1}]$, $E_s'(\lambda)$ is the exoatmospheric spectral irradiance from the Sun in units of $[Wcm^{-2}\mu m^{-1}]$, $\tau_1(\lambda)$ is the transmission through the atmosphere along the Sun-target path, θ is the angle from the surface normal to the Sun, F is the fraction of the spectral irradiance from the sky ($E_d(\lambda)$), incident on the target (*i.e.,* not blocked by adjacent objects), sometimes called shape factor, $\tau_2(\lambda)$ is the transmission along the target-sensor path, $r(\lambda)$ is the spectral reflectance factor for the target of interest (*i.e.,* $r(\lambda)/\pi$ is the bidirectional reflectance $[sr^{-1}]$), $L_u(\lambda)$ is the spectral path radiance $[Wcm^{-2}sr^{-1}\mu m^{-1}]$, and $\beta_p(\lambda)$ is the normalized spectral response of the p^{th} spectral channel of the sensor under study where

$$\beta_p(\lambda) = \frac{\beta_p'(\lambda)}{\int \beta_p'(\lambda)\,d\lambda} \qquad (2)$$

with $\beta_p'(\lambda)$ being the peak normalized spectral response of the p^{th} channel. Schott [2] also describes how the MODTRAN radiative transfer code [3] can be used to solve for each of the radiometric terms in Eq. (1) (*i.e.,* $E_s'(\lambda)$, $\tau_1(\lambda)$, $\tau_2(\lambda)$, $E_d(\lambda)$, and $L_u(\lambda)$) given a set of atmospheric and illumination descriptors. Once the terms are solved for, the spectral radiance target vector $\mathbf{x}$ observed by a *p*-channel sensor can be expressed as

$$\mathbf{x} = [L_1(\lambda), L_2(\lambda), \ldots, L_p(\lambda)]^T. \qquad (3)$$

In practice a *family* of radiance vectors is usually generated to account for lack of knowledge about the atmospheric, illumination and viewing conditions. This is accomplished by varying the inputs to MODTRAN to span a range of variables. In doing so, a wide range of potential target spectral vectors spanning a *target space* can be generated from a single target reflectance spectrum. In general, many of the input parameters to MODTRAN are usually know at the time of image acquisition or can be reasonably estimated (*e.g.,* atmospheric and aerosol model, day of year, location, time of day, etc.). For this research, emphasis is placed on varying unknown MODTRAN parameters such as visibility, water vapor scale factor and ground topography. In the case of water vapor scale factor, a physics based atmospheric compensation algorithm can be used to estimate per pixel total column water vapor which can then be converted to an appropriate range of scale factors. In addition to MODTRAN input parameters, terms such as target orientation and shape factor (F) are also varied. Details on the importance these parameters have on derived target spaces and detection can be found in the literature [4].

2.2. Structured Detection and Infeasibility Metric

If the target and background spaces are described using geometric techniques then the application of a detector based on vector geometry is most appropriate. One such algorithm that relies on (orthogonal) projections is the Orthogonal Subspace Projection (OSP) detector [5]. This can be expressed to include input from *target spaces* such that we have

$$T_{PBosp}(\mathbf{x}) = \frac{\|\mathbf{P_T}\mathbf{P_B^\perp}\mathbf{x}\|}{\|\mathbf{P_T}\mathbf{P_B^\perp}\mathbf{t}_{avg}\|} \qquad (4)$$

where $\mathbf{P_T} = \mathbf{T}\mathbf{T}^\dagger$ where $\mathbf{T}^\dagger$ is the pseudo-inverse of $\mathbf{T}$ defined as $\mathbf{T}^\dagger = (\mathbf{T}^T\mathbf{T})^{-1}\mathbf{T}^T$ and $\mathbf{P_B^\perp} = \mathbf{I} - \mathbf{B}\mathbf{B}^\dagger$. Matrices $\mathbf{T}$ and $\mathbf{B}$ are matrices comprised of endmembers (in columns) that span the target and background subspaces, respectively. The vector $\mathbf{t}_{avg}$ is the average target space spectrum.

The structured infeasibility projector (SIP) provides for a measure of un-target-like behavior by projecting the test pixel onto the subspace orthogonal to the target space and is expressed as

$$T_{SIP}(\mathbf{x}) = ||\mathbf{P_T^\perp}\mathbf{x}|| \qquad (5)$$

where $\mathbf{P_T^\perp} = \mathbf{I} - \mathbf{T}\mathbf{T}^\dagger$. The detector of Eq. (4) and SIP metric of Eq. (5) form the Physics Based-Structured InFeasibility Target-detector (PB-SIFT) which produces a two dimensional decision space where probable targets have large abundances and low SIP scores. This concept of using an added "infeasibility" metric similar to what the SIP produces was motivated by the original work of Boardman [6]. Here, the developed infeasibility concept was stochastic in nature where in this research we set out to develop a geometric equivalent. This metric can also be extended to include the joint statistics of target and background spaces [4].

Two other detectors were used in this research as a means of comparison to the PB-SIFT algorithm. The spectral angle mapper (SAM) generates a test statistic based on the angle between the target and image pixel vectors assuming a target pixel has been manually identified in the scene. The spectral matched filter (SMF) normalizes the target and image pixel product with an image wide covariance estimate, $\mathbf{\Sigma}$. That is

$$T_{SMF}(\mathbf{x}) = (\mathbf{t} - \boldsymbol{\mu}_b)^T\mathbf{\Sigma}^{-1}(\mathbf{x} - \boldsymbol{\mu}_b) \qquad (6)$$

where $\boldsymbol{\mu}_b$ is the mean of the background. This algorithm also assumes the target vector has been identified in the scene or that the scene has been atmospherically compensated and the target spectrum is known from a reflectance library.

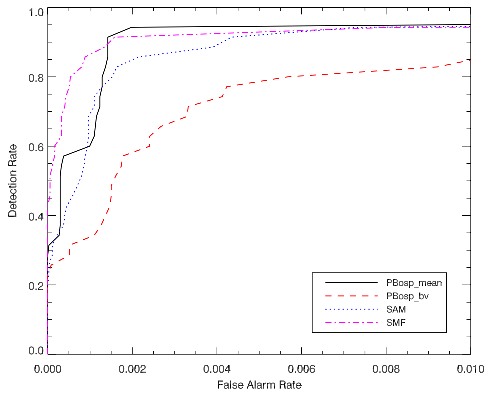

Fig. 1. Generated ROC curves for a fully sunlit target in an open field.

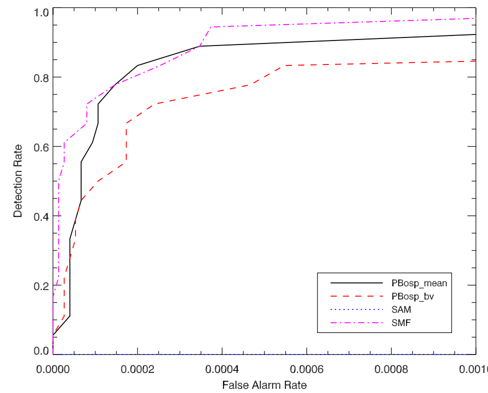

Fig. 2. Generated ROC curves for a target fully concealed by tree canopy in a forested region.

3. RESULTS

All the previously discussed algorithms were applied to two different HYDICE flight lines. The target of interest was a green panel that was placed in an open field in one flight line and then moved into a forested region obscured by tree canopy in a different flight line. The PB-SIFT algorithm was applied to calibrated radiance data while the SAM and SMF algorithms were applied to atmospherically compensated data using the Empirical Line Method (ELM). Target spaces were constructed by varying 4 visibility values, 3 elevation values, 5 water vapor scalar factor values, 3 target orientation values, and 1 to 3 shape factor values, which depended on whether or not the target was obscured. The target and background spaces were then represented using endmembers found using the Maximum Distance method (MaxD) [7] and used in Eq. (4) and (5).

The results of identifying 35 full and mixed target pixels from the sunlit scene can be seen in Figure 1 where we have used two implementations of the PBosp algorithm. One approach characterized the target space using 7 endmembers (PBosp_bv) while the other approach represented the target space using only the mean vector (PBosp_mean). We immediately see that the physics based approach can perform as well as the SAM and SMF algorithms, which rely on atmospheric compensation. Figure 2 shows a similar trend for the case when the target was placed under tree canopy in a forested area. However, it is noted that the SAM algorithm performs extremely poor here and shows up at the bottom of the plot as zero detects.

When we combine the PBosp and SIP results, we generate 2 dimensional decision spaces like those in Figures 3 and 4. Here we see that most pixels have low abundances and are associated with the background. Interesting pixels tend to manifest themselves outside this background distribution. If we simply set a threshold based on the detector test statistic (abundance) only, we can see that we will incur many

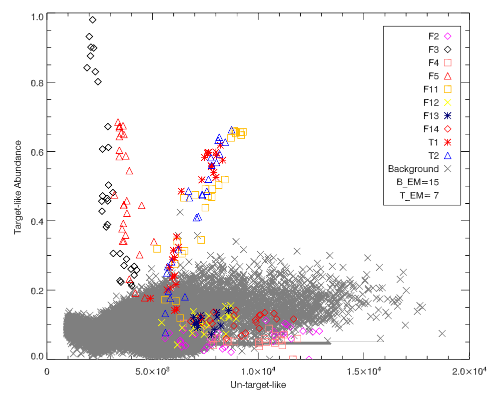

Fig. 3. Two dimensional decision space created using a detector with an added infeasibility metric, as applied to sunlit target imagery.

false alarms for both the fully sunlit and obscured targets. However, we can mitigate these false alarms and therefore improve performance by setting an additional constraint for the SIP values on the x-axis. If we apply this method of improvement to the PBosp_bv case we get the results shown in Figures 5 and 6. As we shift the threshold to lower SIP values we can see the algorithms performance increasing to the point where it now outperforms all algorithms for both levels of target concealment.

4. CONCLUSIONS

The research presented in this paper explored new methods of improving target detection using the concept of physics based modeling. The work builds upon an original body of work related to detection using illumination invariant subspaces. In this paper we refined the process of creating target spaces as well as developed a detector that could adapt to such target

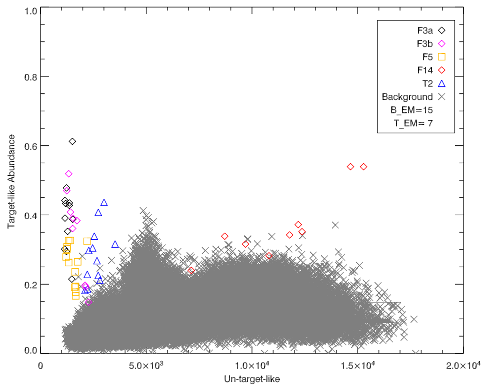

Fig. 4. Two dimensional decision space created using a detector with an added infeasibility metric, as applied to canopy-obscured target imagery.

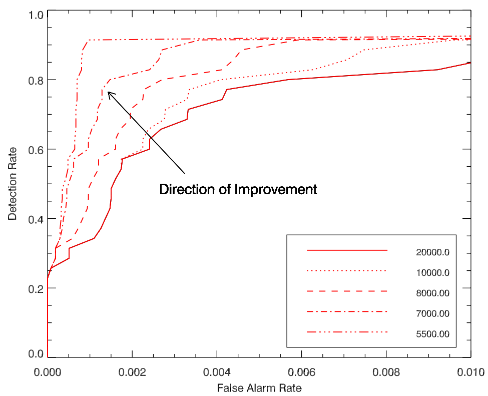

Fig. 5. Improved PBosp_bv algorithm performance by varying the SIP threshold for the sunlit target imagery.

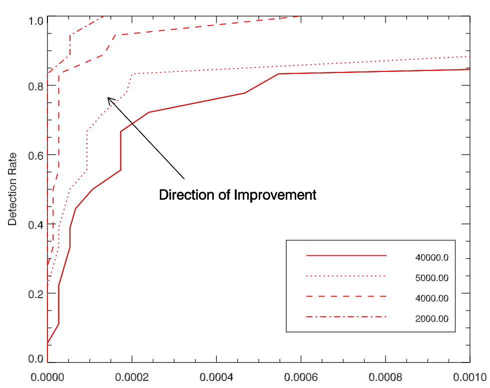

Fig. 6. Improved PBosp_bv algorithm performance by varying the SIP threshold for the canopy-obscured target imagery.

spaces. In addition, we extended the detection process to incorporate an added geometric infeasibility measure. The algorithms were tested on HYDICE data where results showed that the physics based approach performs as well as methods that used (research grade) atmospherically compensated imagery. Furthermore, the PB-SIFT approach actually *outperformed* both the SAM and SMF algorithms for both the sunlit and canopy-obscured test imagery. Future efforts will address the inclusion of sensor noise and calibration errors into the target space as well as its impact on detector performance. Additionally, a criteria needs to be established on where to set the decision boundary in addition to further developing the SIP by incorporating the joint statistics of target and background spaces.

5. REFERENCES

[1] G. Healey and D. Slater. Models and methods for automated material identification in hyperspectral imagery acquired under unknown illumination and atmospheric conditions. *IEEE Transactions on Geoscience and Remote Sensing*, 37(6):2706–2717, November 1999.

[2] J.R. Schott. *Remote Sensing: The Imaging Chain Approach*. Oxford University Press, New York, 1997.

[3] A. Berk, L.S. Bernstein, and D.C. Robertson. MODTRAN: A moderate resolution model for LOWTRAN 7. Technical Report GL-TR-89-0122, Air Force Geophysics Laboratory, Hanscom AFB, MA, 1988.

[4] E.J. Ientilucci and J.R. Schott. Target detection in a structured background environment using an infeasibility metric in an invariant space. In Paul E. Lewis Sylvia S. Shen, editor, *Proc. SPIE, Algorithms and Technologies for Multispectral,Hyperspectral, and Ultraspectral Imagery XI*, volume 5806, pages 491–502, Orlando, FL, April 2005.

[5] J.C. Harsanyi and C.I. Chang. Hyperspectral image classification and dimensionality reduction: An orthogonal subspace projection approach. *IEEE Transactions on Geoscience and Remote Sensing*, 32(4):779–785, July 1994.

[6] J. W. Boardman. Leveraging the high dimensionality of AVIRIS data for improved sub-pixel target unmixing and rejection of false positives: mixture tuned matched filtering. In Robert O. Green, editor, *Summaries of the Seventh Annual JPL Airborne Geoscience Workshop*, volume 1 of *JPL Publication 97-21*, page 55, Pasadena, California, January 1998.

[7] K. Lee. *A sub-pixel scale target detection algorithm for hyperspectral imagery*. PhD dissertation, Rochester Institute of Technology, 54 Lomb Memorial Drive, Rochester, NY, 2003.